

Organic-Capped ZnO Nanocrystals: Synthesis and n-Type Character

Moonsub Shim[†] and Philippe Guyot-Sionnest*

Contribution from The James Franck Institute, University of Chicago, Chicago, Illinois 60637

Received June 1, 2001

Abstract: Wurtzite ZnO nanocrystals capped with trioctylphosphine oxide or alkylamines are synthesized and characterized. These ZnO nanocrystals can be made n-type either by electron transfer doping from reducing species in solution or by above band gap photoexcitation with a UV lamp. The n-type nanocrystals exhibit a strong intraband infrared absorption, an extensive bleach of the interband band-edge absorption, and a complete quenching of the photoluminescence.

Introduction

Semiconductor nanocrystal colloids are receiving much attention owing to their novel optical and electronic properties^{1,2} with applications in solar cells³ and light emitting diodes.⁴ The readily exchangeable organic capping moieties provide the versatility with which the unique properties arising in the nanometer size scale can be manipulated.⁵ Recent advances in charge transfer doping to make n-type nanocrystal colloids⁶ further enhance their potential as components of future nanotechnology.

A key ingredient for the study and applications of nanocrystals is a reliable synthetic route to high-quality materials. While nanocrystal colloids can be synthesized by a variety of methods, the most successful in terms of controlled size, size-dispersion, readily exchangeable surface properties, and crystallinity has been the high-temperature decomposition of organometallic precursors in a coordinating solvent developed by Murray and co-workers.⁵ Modifications of this method have allowed the synthesis of many different materials including InP,⁷ ZnSe,⁸ Co,⁹ and FePt¹⁰ nanocrystals. However, there has not been an equivalent success in the synthesis of oxide nanocrystals. Although TiO₂ nanocrystals capped with trioctylphosphine oxide (TOPO) prepared in a similar manner have recently been reported,¹¹ this system does not exhibit quantum confinement.

Analogous to bulk semiconductors, another important aspect in broadening the applicability of nanometer scale semiconductors is the ability to control the Fermi level via n- and p-type

materials. We have recently shown that electron injection into the quantum-confined states of semiconductor nanocrystals (CdSe, ZnO, CdS) is possible, with a stability that depends on the material and the degree of confinement.⁶ Electrochemical electron injection also provides reversible optical changes, switched on and off by an external potential.¹²

Here, we report on the details of the synthesis of ZnO nanocrystals capped with TOPO or alkylamines. We further report that above band gap excitation leads to the same spectroscopic changes as electron transfer with a very long-lived electron in the lowest conduction band quantum state 1S_e.

Experimental Section

ZnO nanocrystals are prepared by using standard airless techniques. To 4 mL of degassed octylamine bubbled O₂ is bubbled for ~2 min. While continuing to bubble O₂, 150 μL of diethylzinc in 4 mL of anhydrous decane is injected with the tip of the needle submerged in solution to prevent reaction of diethylzinc with gaseous O₂ above the reaction solution. O₂ is allowed to bubble for another ~30 s, then the reaction mixture is loaded into a 10 mL syringe and rapidly injected into 6 g of degassed trioctylphosphine oxide (TOPO) at 200 °C under Ar atmosphere (the flash point of TOPO is ~230 °C and the TOPO reaction flask must be maintained under Ar atmosphere at high temperature). Higher temperature injection leads to smaller amounts of ZnO nanocrystals possibly due to O₂ gas evolution before ZnO formation. Upon injection of Zn/O reagent, temperature drops to ~140 °C. The growth of the nanocrystals is carried out at temperatures between 150 and 180 °C. It should be noted that at these temperatures with a narrow size dispersion (i.e. $\sigma \leq 10\%$), growth of ZnO nanocrystals becomes exceedingly slow when the first absorption maximum reaches ~330 nm (~3 nm in diameter). Further growth can be carried out with slow addition of more Zn/O precursor prepared in octylamine. However, broadening of the exciton absorption is observed as further growth occurs.

While ZnO nanocrystals prepared from zinc salts in alcoholic solutions continue to grow after preparation,^{13,14} in the high-temperature organometallic synthesis, TOPO prevents further growth once heat is removed. The ZnO nanocrystals are readily precipitated with methanol or acetonitrile and redispersed in solvents such as CHCl₃ or hexane without any irreversible aggregation or growth. Size-selective precipitation with solvent/nonsolvent combination can be carried out as for CdSe nanocrystals. ZnO nanocrystals can also be grown directly in amines by slow heating of the reaction mixture to ~60 °C instead of injecting Zn/O precursor into TOPO. However, octylamine- and dodecylamine-

* Address correspondence to this author.

[†] Present address: Department of Chemistry, Stanford University, Stanford, CA 94305.

- (1) Nirmal, M.; Brus, L. E. *Acc. Chem. Res.* **1999**, *32*, 407.
- (2) Kastner, M. A. *Phys. Today* **1993**, *24*, Ashoori, R. C. *Nature* **1996**, *379*, 413.
- (3) O'Regan, B.; Grätzel, M. *Nature* **1991**, *353*, 737.
- (4) Colvin, V. L.; Schlamp, M. C.; Alivisatos, A. P. *Nature* **1994**, *370*, 354. Dabbousi, B. O.; Bawendi, M. G.; Onitsuka, O.; Rubner, M. F. *Appl. Phys. Lett.* **1995**, *66*, 1316.
- (5) Murray, C. B.; Norris, D. J.; Bawendi, M. G. *J. Am. Chem. Soc.* **1993**, *115*, 8706.
- (6) Shim, M.; Guyot-Sionnest, P. *Nature* **2000**, *407*, 981.
- (7) Micic, O. I.; Curtis, C. J.; Jones, K. M.; Sprague, J. R.; Nozik, A. J. *J. Phys. Chem.* **1994**, *98*, 4966.
- (8) Hines, M. A.; Guyot-Sionnest, P. *J. Phys. Chem. B* **1998**, *102*, 3655.
- (9) Dinega, D. P.; Bawendi, M. G. *Angew. Chem., Int. Ed. Engl.* **1999**, *38*, 1788. Sun, S.; Murray, C. B. *J. Appl. Phys.* **1999**, *85*, 4325.
- (10) Sun, S.; Murray, C. B.; Weller, D.; Folks, L.; Moser, A. *Science* **2000**, *287*, 1989.
- (11) Trentler, T.; Denler, T. E.; Bertone, J. F.; Agrawal, A.; Colvin, V. L. *J. Am. Chem. Soc.* **1999**, *121*, 1613.

(12) Wang, C.; Shim, M.; Guyot-Sionnest, P. *Science* **2001**, *291*, 2390.

(13) Spanhel, L.; Anderson, M. A. *J. Am. Chem. Soc.* **1991**, *113*, 2826.

(14) Meulenkamp, E. A. *J. Phys. Chem. B* **1998**, *102*, 5566.

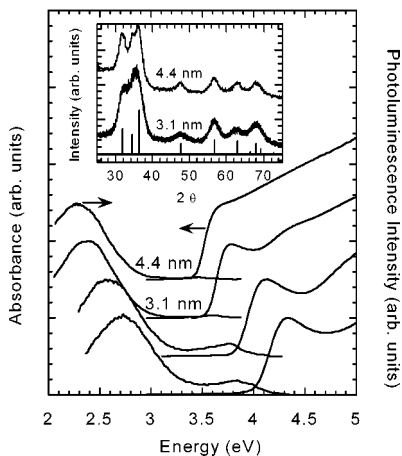


Figure 1. Absorption and photoluminescence spectra of different sizes of ZnO nanocrystals. The lower two sets of spectra are ZnO nanocrystals capped with octylamine and the upper two sets are those capped with TOPO. The sizes indicated are the average diameters. The inset shows the powder X-ray diffraction patterns of TOPO-capped ZnO nanocrystals along with wurtzite ZnO diffraction lines.

capped ZnO nanocrystals continue to grow slowly at room temperature, resulting in a white precipitate in several days to weeks depending on the initial size and size-distribution of the nanocrystals. The ZnO nanocrystals are characterized by UV/Vis absorption (HP-8453), photoluminescence (PL) with a LS-50 Perkin-Elmer spectrometer, transmission electron microscopy (TEM) with a Philips CM120 operating at 120 keV, and powder X-ray diffraction. Under the TEM, the nanocrystals appear roughly spherical, and the diameters (± 0.5 nm) are determined by visual inspection of a field of nanocrystals on the TEM photographs. The corresponding absorption spectra for a given size agree within the error bars with previous literature data.¹⁴

Charge transfer from sodium biphenyl reagent is carried out in the manner described in ref 6. The ZnO nanocrystals are precipitated once with methanol from the growth solution. The precipitate is dried under vacuum and transferred in a dry glovebox (<5 ppm O_2), before being redissolved in dry 2,2,4,4,6,6,8,8-heptamethylnonane (HMN). Standard IR liquid cells are filled in the glovebox. The solvent tight cell can then be taken out of the glovebox for optical characterization. Samples are exposed to a hand-held UV lamp or Xe arc lamp and kept in the dark between measurements. We emphasize that the samples must be handled in the glovebox. Simply filling the sample cell in ambient atmosphere prevents the observation of UV-induced optical changes.

Results

ZnO is a direct band-gap semiconductor with an electron effective mass of $\sim 0.24 m_e$ and a hole effective mass of $\sim 0.59 m_e$. The three valence bands are split by the crystal field (~ 40 meV) but not significantly by spin-orbit coupling. The small masses lead to an expected strong size dependence of the band edge absorption¹⁵ that has been previously reported.^{13,14} Figure 1 shows the room temperature UV/Vis absorption and PL spectra of four different sizes of ZnO nanocrystals as grown, without further size selection, showing the effect of quantum confinement. The lower two spectra are of ZnO nanocrystals grown directly in octylamine. Powder X-ray diffraction confirms the wurtzite structure. From TEM, the size-distribution of the ~ 3.1 nm diameter samples shown in Figure 1 is $\sim 10\%$. The first exciton feature ($1S_h-1S_e$) becomes better resolved as the size is reduced, but temperature has only a little effect on the spectral widths. The second exciton feature ($1P_h-1P_e$) is not well-resolved, which may be due to the lifted degeneracy of hole and electron P-states arising from the shape or crystal-field.

(15) Brus, L. E. *J. Chem. Phys.* **1984**, *80*, 4403.

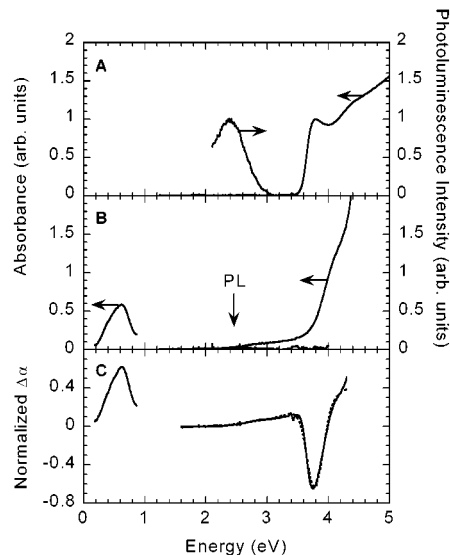


Figure 2. Comparison of the absorption and photoluminescence spectra of TOPO-capped ZnO nanocrystals (3.1 nm average diameter) before (A) and after (B) charge-transfer doping with sodium biphenyl. The difference spectrum normalized to the first exciton maximum of the spectrum before UV is shown in part C and is fitted to one Gaussian and a rising tail of the form $A(E - E_g)^{2.5}$, where A is a constant and E_g is the bulk band gap. The dotted line is the fit.

Both TOPO- and amine-capped ZnO nanocrystals exhibit broad Stokes shifted emission. The large Stokes shift implies a trapping process. The strong size dependence of the emission peak position suggests that one carrier is in a quantum-confined state. On the basis of the size dependence of the fluorescence energy, it has been assigned to a transition from the conduction band state to a deep hole trap, about 1 eV above the valence band, induced by an oxygen vacancy.^{16,17} This is in accord with our observation, noting that the TOPO-capped ZnO nanocrystals in anhydrous and oxygen-free solution are probably oxygen deficient. There have been observations of weak near band-edge emission, enhanced upon UV irradiation of deaerated solutions for ZnO nanocrystals prepared in alcoholic solutions.^{16,18} No detectable band edge emission is observed in the TOPO-capped ZnO nanocrystals, in anhydrous and oxygen-free solution, either upon UV irradiation or after electron injection.

Figures 2 and 3 compare the absorption and photoluminescence properties of two samples of TOPO-capped ZnO nanocrystals of ~ 3.1 nm diameter before and after charge transfer (Figure 2) or before and after UV exposure (Figure 3). There is a bleach of the interband exciton absorption, a complete quenching of the photoluminescence, and a very strong mid-IR absorption at ~ 0.5 eV with integrated intensity as large as the exciton absorption bleach. These optical changes are similar to those observed for n-type CdSe nanocrystals.^{6,12,21}

In the 3.1 nm nanocrystal, the peak exciton is at ~ 3.7 eV, 0.5 eV larger than the room-temperature ZnO band gap of $E_g \sim 3.2$ eV. Neglecting correlation, which is valid at a radius smaller than twice the Bohr radius,¹⁹ the exciton energy is the sum of the band gap energy, E_g , the electron and hole

(16) van Dijken, A.; Meulenkamp, E. A.; Vanmaekelbergh, D.; Meijerink, A. *J. Phys. Chem. B* **2000**, *104*, 1715.

(17) Monticone, S.; Tufeu, R.; Kanaev, A. V. *J. Phys. Chem. B* **1998**, *102*, 2854.

(18) Koch, U.; Fojtik, A.; Weller, H.; Henglein, A. *Chem. Phys. Lett.* **1985**, *122*, 507.

(19) Kayanuma, Y.; Momiji, H. *Phys. Rev. B* **1990**, *41*, 10261.

(20) Khurgin, J. *Appl. Phys. Lett.* **1993**, *62*, 1390.

(21) Shim, M.; Wang, C.; Guyot-Sionnest, P. *J. Phys. Chem. B* **2001**, *105*, 2369.

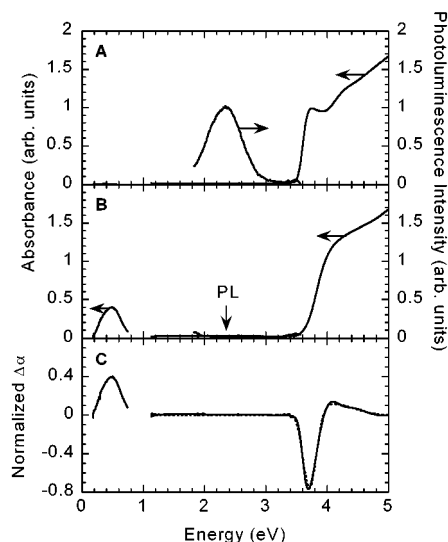


Figure 3. Comparison of the absorption and photoluminescence spectra of TOPO-capped ZnO nanocrystals (3.1 nm average diameter) in HMN before (A) and after (B) 15 min of exposure to a hand-held UV lamp. The difference spectrum normalized to the first exciton maximum of the spectrum before UV is shown in part C and is fitted to two Gaussians (dotted line).

confinement energy, and their Coulomb interaction.¹⁵ The ZnO optical dielectric constant is $\epsilon = 3.7$. The parabolic effective mass approximation with infinite boundary conditions¹⁵ applied to a ZnO nanocrystal of ~ 3 nm diameter leads to an exciton with 0.5 eV excess energy, arising from ~ 0.65 eV of electron confinement energy, ~ 0.3 eV of hole confinement energy, and ~ -0.45 eV of Coulomb attraction. In a spherical quantum dot with infinite boundary potential, the dominant transition for an electron in the $1S_e$ state is to the $1P_e$ state, and the $1S_e-1P_e$ spacing is similar to the $1S_e$ confinement energy. The observed IR transition peaks around 0.5 eV, which is therefore consistent with the $1S_e-1P_e$ assignment. This assignment is strongly supported by the oscillator strength of the IR transition, since it is similar to the exciton as it should be for the intraband transition $1S_e-1P_e$.²⁰ The large oscillator strength of the intraband transition has previously been discussed in n-type^{6,23,21} and photoexcited²² CdSe nanocrystals.

An alternative assignment of the IR transition is to invoke a trap state. In previous literature, electron transfer in colloidal semiconductor nanocrystals in aqueous or alcohol solution was justifiably considered to result in rapid electron trapping at surface sites. The resulting surface charge could explain a bleach of the exciton peak, via Stark shift and broadening for example, without the need to invoke $1S_e$ electron occupation. To be consistent with the IR energy observed here, the electron trap could be close to the bottom of the conduction band allowing transition to the $1S_e$ state. However, the existence of a trap at this position is contrary to the current understanding of the visible emission. Another possibility is a “shallow” trap just below $1S_e$ with a transition to $1P_e$. In general, the optical absorption cross-sections of transitions involving localized trap states are small or undetectable because of the small overlap of the wave function of the localized trap with the delocalized states. As a consequence, the oscillator strength from an electron in a trap state should be spread among many transitions leading to a broad weak continuum, difficult to detect. The large

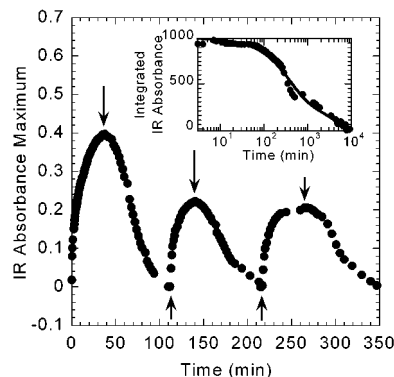


Figure 4. Time evolution of the IR intraband absorption of TOPO-capped ZnO nanocrystals upon UV excitation. Up-arrows indicate the times at which the hand-held UV lamp is switched on and the down-arrows are the times at which it is turned off. When normalized, the three decay curves overlap nearly identically. The inset shows the decay of the IR absorption after excitation with the Xe arc lamp. Depending on the intensity of the UV source, the duration of the n-type character under ambient conditions can be varied. The line in the inset is a fit to two-exponential decay. The longer component has a lifetime over 2 days.

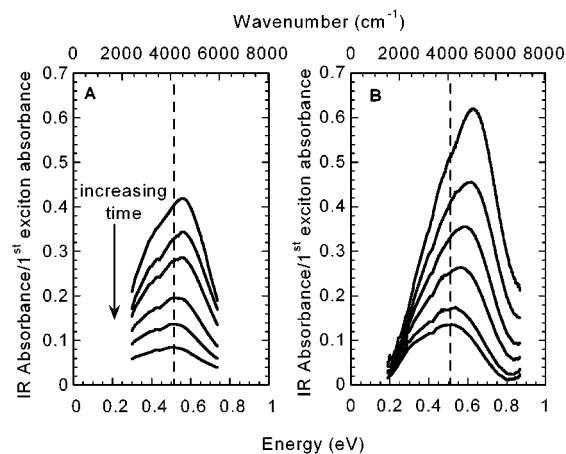


Figure 5. Comparison of the intraband IR absorption of n-type ZnO nanocrystals made by photoexcitation by an Xe arc lamp (A) and charge-transfer doping (B). The spectra are normalized to each sample’s optical density at the first exciton absorption maximum. Initially, the IR absorption maximum appears at 0.55 eV for UV-excited nanocrystals and at 0.64 eV for charge-transfer doped nanocrystals. However, the final IR absorption peak positions are the same in both cases.

observed IR cross-section then requires this “shallow” trap to be highly delocalized, hence undistinguishable from the $1S_e$ state. Therefore, on the basis of the current understanding of the visible fluorescence, the correct energy, and cross-section of the IR transition, we conclude that the IR transition is indeed the intraband $1S_e-1P_e$ transition.

The unexpected feature exhibited by the ZnO nanocrystals is that weak *cw* UV-excitation is sufficient to place an electron in the $1S_e$ state for an extended time. This contrasts with CdSe nanocrystals for which photoexcitation also leads to electrons in the $1S_e$ state but at most for ~ 1 ms when the surface is modified with specific hole traps.^{23,24} The inset in Figure 4 shows the decay of the mid-IR absorption under ambient conditions after ZnO nanocrystals have been exposed to the Xe arc lamp for 5 min. Simply switching on/off a hand-held UV lamp with lower intensity leads to reversible IR absorption

(22) Guyot-Sionnest, P.; Hines, M. A. *Appl. Phys. Lett.* **1998**, *72*, 686.

(23) Shim, M.; Shilov, S. V.; Braiman, M. S.; Guyot-Sionnest, P. *J. Phys. Chem. B* **2000**, *104*, 1494.

(24) Ginger, D. S.; Dhoot, A. S.; Finlayson, C. E.; Greenham, N. C. *Appl. Phys. Lett.* **2000**, *77*, 2816.

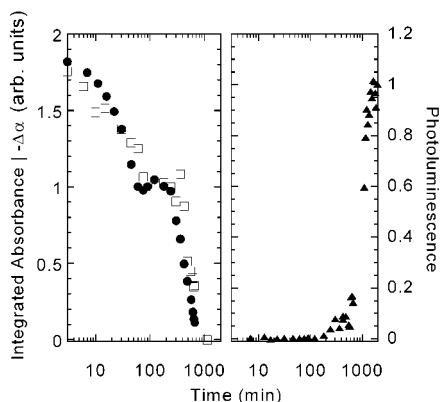


Figure 6. Logarithmic time evolution of the intraband IR absorption (filled circles), interband exciton absorption bleach (open squares), and photoluminescence (filled triangles) of charge-transfer doped ZnO nanocrystals. The IR absorption and exciton bleach are normalized such that the plateau is at one.

changes as shown in Figure 3. In fact, the effect was first noticed while monitoring the fluorescence in the weak UV light of the fluorescence spectrometer. Note that samples irradiated at room temperature and cooled to 10 K display the IR absorption indefinitely, while hole-burning spectra⁶ exhibit a narrow (<30 cm^{-1}) IR homogeneous line.²⁵

There are two differences between charge transfer and UV-excitation. Nanocrystals prepared by charge transfer exhibit an absorption tail below the band-edge, also seen for CdSe nanocrystals.^{6,21} We currently attribute the tail to transitions involving occupied surface states that may arise from surface modifications in the strongly reducing solution. The second difference, seen in all samples investigated, is that charge transfer doped nanocrystals can exhibit a larger bleach of the exciton and a stronger mid-IR absorption as shown in Figure 5. Both sets of spectra are normalized to the absorbance of the unperturbed exciton peak. As shown in Figure 6A, the nearly matching decays of the IR absorption and of the exciton bleach for charge-transfer doped nanocrystals exhibit a plateau. We find that the IR absorption at the plateau is similar in its normalized magnitude and peak energy to the maximum response obtained with UV-excitation. These results concur to suggest that reduction by sodium biphenyl can place more electrons on average in the conduction band than UV-excitation.

The observations are rationalized by realizing that *cw* UV-excitation should only bring the nanocrystals in the one-electron reduced state because of fast Auger recombination. Indeed, n-type nanocrystals exhibit complete luminescence quenching due to fast Auger recombination of the photoexcited electron–hole pair. Since Auger recombination is much faster than the luminescence it must also be much faster than the hole-trapping or scavenging process (which one is unknown at present) that leads to the UV-induced n-type character in the first place. Therefore, *cw* UV-excitation of the nanocrystal should lead to at most one conduction electron, in contrast to charge transfer doped nanocrystals which can have up to two electrons in the $1S_e$ state.

The plateau observed in the decays of the IR absorption and exciton bleach in Figure 6A is attributed to different one- and two-electron reduction potentials arising from charging energy and the Coulomb repulsion between the electrons. This two-step oxidation process has not been seen so far in n-type CdSe nanocrystals,²¹ but the smaller size of the ZnO nanocrystals and the smaller *dc* dielectric constant ($\epsilon(0) \sim 8.5$) may explain why charging and Coulomb repulsion are more significant here.

Conclusions

ZnO nanocrystal colloids capped with TOPO or amines are made by organometallic synthesis with a narrow size-distribution. The long-term stability and the well-controlled sizes of the nanocrystals will facilitate studies of the quantum states and of the nature of the fluorescence. We report here that the ZnO nanocrystals can be made n-type by charge-transfer doping and by above band gap *cw*-photoexcitation. As in n-type CdSe nanocrystals,²¹ n-type ZnO nanocrystals exhibit strong mid-IR absorption corresponding to an intraband transition along with a concurrent bleach of the interband exciton absorption, while the visible photoluminescence is quenched.

Acknowledgment. This work was funded by the National Science Foundation under grant No. DMR-9731642. We made use of the MRSEC Shared Facilities supported by the National Science Foundation under grant No. DMR-9400379.

JA0163321

(25) Shim, M. Ph.D. Thesis, University of Chicago, November 2000.